THE JOURNAL OF BIOLOGICAL CHEMISTRY VOL. 288, NO. 24, pp. 17225–17237, June 14, 2013

The DNAJB6 and DNAJB8 Protein Chaperones Prevent Intracellular Aggregation of Polyglutamine Peptides*

Received for publication, February 5, 2013, and in revised form, April 18, 2013 Published, JBC Papers in Press, April 23, 2013, DOI 10.1074/jbc.M112.421685

Judith Gillis[‡1], Sabine Schipper-Krom[‡1], Katrin Juenemann[‡], Anna Gruber[‡], Silvia Coolen[‡], Rian van den Nieuwendijk[§], Henk van Veen[‡], Hermen Overkleeft[§], Joachim Goedhart[¶], Harm H. Kampinga[‖], and Eric A. Reits[‡2]

From the [‡]Department of Cell Biology and Histology, Academic Medical Center, Amsterdam 1105AZ, The Netherlands, the [§]Department of Bio-Organic Synthesis, Leiden University, 2333CC, The Netherlands, the [¶]Swammerdam Institute for Life Sciences, University of Leiden, 1090GE, The Netherlands, and the [‖]Department of Cell Biology, University Medical Center Groningen, Groningen, Amsterdam 9713AV, The Netherlands

Background: Intracellular aggregation of polyglutamine (polyQ) proteins can be prevented by the chaperones DNAJB6 and DNAJB8.
Results: DNAJB6 and DNAJB8 prevent the aggregation of pure polyQ peptides.
Conclusion: The polyQ tract is sufficient for DNAJB6 and DNAJB8 to prevent aggregation.
Significance: By interacting with polyQ fragments, DNAJB6 and DNAJB8 reduce polyQ protein aggregation and may be potential therapeutic targets in polyQ disorders.

Fragments of proteins containing an expanded polyglutamine (polyQ) tract are thought to initiate aggregation and toxicity in at least nine neurodegenerative diseases, including Huntington's disease. Because proteasomes appear unable to digest the polyQ tract, which can initiate intracellular protein aggregation, preventing polyQ peptide aggregation by chaperones should greatly improve polyQ clearance and prevent aggregate formation. Here we expressed polyQ peptides in cells and show that their intracellular aggregation is prevented by DNAJB6 and DNAJB8, members of the DNAJ (Hsp40) chaperone family. In contrast, HSPA/Hsp70 and DNAJB1, also members of the DNAJ chaperone family, did not prevent peptide-initiated aggregation. Intriguingly, DNAJB6 and DNAJB8 also affected the soluble levels of polyQ peptides, indicating that DNAJB6 and DNAJB8 inhibit polyQ peptide aggregation directly. Together with recent data showing that purified DNAJB6 can suppress fibrillation of polyQ peptides far more efficiently than polyQ expanded protein fragments *in vitro*, we conclude that the mechanism of DNAJB6 and DNAJB8 is suppression of polyQ protein aggregation by directly binding the polyQ tract.

Polyglutamine (polyQ)[3] disorders are a group of dominantly inherited, progressive neurodegenerative disorders. These disorders are caused by expansion of the polyQ tract within coding regions of unrelated proteins. At least nine different polyQ disorders are known, including Huntington´s disease (1). These disorders are characterized by atrophy of certain regions in the brain and the presence of intracellular aggregates that are thought to initiate disease, although neither the precise toxic species nor the cause of aggregation initiation are fully understood. Several studies showed that these aggregates contained not only the full-length disease-related protein but also shortened fragments, including the expanded polyQ tract (2–4). Furthermore, it was shown that truncated forms of huntingtin (Htt), ataxin 3, ataxin 7, atrophin 1, and the androgen receptor containing the expanded polyQ tract, are more aggregation-prone and enhance toxicity (5–11). Although proteasomes are able to degrade polyQ-containing proteins (12–15), they may not be able to cleave within polyQ tracts *in vitro* (16). As a consequence, polyQ peptides may be released upon proteasomal degradation of expanded polyQ proteins. Similar polyQ peptides may be directly generated in related disorders, such as SCA8 and Huntington's disease like-2 (HDL2), which are thought to be initiated by polyQ peptides generated by antisense transcription that cause intranuclear inclusions (9, 17). When mimicking polyQ peptide generation in living cells, we observed that expression of expanded polyQ peptides is sufficient to induce aggregation and toxicity in cells (18) and that expression of polyQ stretches alone causes toxicity in *Drosophila* (19).

Aggregates or inclusion bodies initiated by expanded polyQ peptides as well as expanded polyQ-containing proteins are decorated with various proteins, such as components of the ubiquitin-proteasome system and heat shock proteins (HSP) (20–26). HSPs can function as molecular chaperones. Many of them are up-regulated under stress conditions, such as heat stress (27, 28), and have been shown to protect cells against heat-induced protein aggregation (29, 30). Heat shock proteins can be classified into a number of families on the basis of their approximate molecular mass and presence of conserved domains (31, 32). The HSPA (Hsp70) family consists of 11

* This work was supported by VENI Grant 91646038 and VIDI Grant 91796315 from NWO-Zon-MW and by a grant from the Hersenstichting (to E. R.), and by Agentschap.nl Grant IOP IGE07004 (to H. H. K.).
[1] Both authors contributed equally to this work.
[2] To whom correspondence should be addressed: Department of Cell Biology and Histology, Academic Medical Center, Meibergdreef 15, 1105 AZ, Amsterdam, The Netherlands. Tel.: 31-20-5666259; E-mail: e.a.reits@amc.uva.nl.
[3] The abbreviations used are: polyQ, polyglutamine; Htt, huntingtin; HSP, heat shock protein; Ub, ubiquitin; FLIM, fluorescent lifetime imaging.

members, whereas the DNAJ (Hsp40) family consists of over 40 members in humans (32). In a recent comparative screen of all members of the HSPA, HSPH (Hsp110), and DNAJ (sub)families, DNAJB6 and DNAJB8 were identified as the two most potent suppressors of aggregation and related toxicity of expanded polyQ proteins (33). When examining the characteristics of these two chaperones in more detail, we now find that DNAJB6 and DNAJB8 can directly suppress aggregation of polyQ peptides generated in living cells. This action is largely dependent on the serine-rich region (SSF-SST) within the C terminus and less dependent on interaction with Hsp70. Intriguingly, expression of DNAJB6 in the nucleus also represses aggregation in the cytoplasm, suggesting that polyQ peptides are kept solubilized in one cellular compartment by these chaperones and remain small enough to travel to the other compartment for subsequent degradation. The ability of DNAJB6 and DNAJB8 to reduce aggregation of expanded polyQ peptides prevents these polyQ peptides from acting as inducers of aggregation and improves their clearance.

EXPERIMENTAL PROCEDURES

DNA Constructs—Generation of GFP-Ub-polyQ constructs was described before (18). However, the initial polyQ peptides started with a Leu residue and a Glu-Thr-Ser-Pro-Arg sequence at the C terminus. This Leu residue was changed into a Gln using QuikChange II site-directed mutagenesis (Stratagene). At the C terminus, a stop codon was introduced directly after the polyQ stretch using site-directed mutagenesis, resulting in GFP-Ub-Q16 and GFP-Ub-Q104, respectively. To insert a tetracysteine (C4) tag after the polyQ tract, a BamHI site was introduced at the N terminus of polyQ peptides using GFP-Ub-Q16/112, where Leu was already changed into a Gln. The C4 tag containing the sequence FLNCCPGCCMEP (34) was obtained by annealing two encoding oligo primers with overhangs compatible with BamHI at the N terminus and XbaI at the C terminus. A C4 tag was inserted into GFP-Ub-polyQ using BamHI and XbaI, thereby generating GFP-Ub-Q17-C4 and GFP-Ub-Q99-C4, respectively.

Plasmids encoding DNAJB6a, DNAJB6b (including H31Q), and DNAJB8 (including H31Q and ΔSSF-SST) in pcDNA5 FRT/TO V5 vectors were described before (33) and were subsequently cloned into either pIRES-DsRed2 (Invitrogen) to generate untagged chaperones or into tagRFP (Evrogen) to generate chaperones N-terminally tagged with red fluorescent protein. DNAJB6b ΔSSF-TST was generated by deleting amino acids 155–195 within DNAJB6b. Htt-exon1-Q103-GFP was provided by Ron Kopito (Stanford University, Stanford, CA), and HSPA1A-GFP was provided by Harm Kampinga (University Medical Center Groningen, Groningen, The Netherlands).

Cell Culture and Transfection—HEK293 cells and the human melanoma cell line Mel Juso were cultured in Iscove's modified Dulbecco's medium (Invitrogen) supplemented with 10% FCS, 25 mM Hepes, 100 units/ml penicillin, 100 μg/ml streptomycin, and 1 mM glutamine (Invitrogen). HeLa cells were cultured in Dulbecco's modified Eagle's medium (Invitrogen) supplemented as described above. HeLa and Mel Juso cells (0.15×10^6) were plated onto glass coverslips (24 mm, Fisher Scientific) in a 6-well plate and were transiently transfected using FuGeneHD (Roche) 24 h after plating. HEK293 cells (0.1×10^6) were seeded in 6-well plates and transiently transfected with polyethylenimine (Polysciences) 24 h after plating.

siRNA Transfection—24 h after seeding, cells were transfected with 50 nM control siRNA or DnaJb6 siRNA, repeated 48 h after seeding with 50 nM control siRNA or DnaJb6 siRNA together with 2.5 μg of plasmid (48-h protein expression). Transfections were done with Lipofectamine 2000 (Invitrogen) and Dharmacon SMARTpool siRNA siGenome DNAJB6 (M-013020-00-0005) and non-targeting siRNA control siGENOME (D-001206-13-20).

Biarsenical Labeling—HeLa cells were transfected with GFP-Ub-Q99-C4 and DNAJB6 or DNAJB8, and biarsenical labeling was performed 72 h after transfection, as described before (34). Briefly, 1 mM ReAsH was preincubated in 10 mM 1,2-ethanedithiol (Sigma) in DMSO for 10 min. Cells were labeled with 1 μM ReAsH in 10 μM 1,2-ethanedithiol in OptiMEM for 45 min at 37 °C, 10% CO_2 in the dark and subsequently washed several times with 1 mM 1,2-ethanedithiol in OptiMEM containing 10% FCS for 30 min at room temperature to remove unbound dyes.

Confocal and FRET-FLIM Microscopy—HEK293T cells were cotransfected with GFP-Ub-polyQ and various chaperones, as indicated in the figure legends, and the percentage of aggregate-positive cells was determined after 72 h. The number of cells containing aggregates in the nucleus, cytoplasm, or both compartments was determined 48 and 72 h after transfection. Confocal microscopy images were obtained 48 h after transfection using a Leica SP2 confocal system equipped with an Ar/Kr laser with a ×63 objective. For fluorescence loss in photobleaching analysis, either a part of the cytoplasm or the whole cell, except for the aggregate, was repeatedly photobleached at full laser power. Fluorescence loss was measured either within the nucleus or within the non-bleached region containing the aggregate, respectively. For fluorescent recovery after photobleaching analysis, fluorescently tagged chaperones trapped in polyQ peptide-induced aggregates were bleached at full laser power, and fluorescence recovery was measured in time. FLIM was carried out after biarsenical labeling of living cells. To reduce interference of autofluorescence by DMEM, a special medium was added to cells (20 mM Hepes (pH 7.4), 137 mM NaCl, 5.4 mM KCl, 1.8 mM $CaCl_2$, 0.8 mM $MgCl_2$, and 20 mM glucose). FLIM was performed using the wide-field frequency domain approach on a home-built instrument (35) using a radio-frequency-modulated image intensifier (Lambert Instruments, model no. II18MD) coupled to a CCD camera (Photometrics HQ) as a detector. A × 40 objective was used for all measurements. The modulation frequency was set to 75.1 MHz. Eighteen phase images with an exposure time of 20–200 ms were acquired in a random recording order to minimize artifacts because of photobleaching (36). From the phase sequence, an intensity image and the phase and modulation lifetime image were calculated using Matlab macros. From this data, the lifetime of individual cells was determined. Subsequently, average phase and modulation lifetimes (± S.D.) were calculated. The FRET efficiency (E) was calculated according to

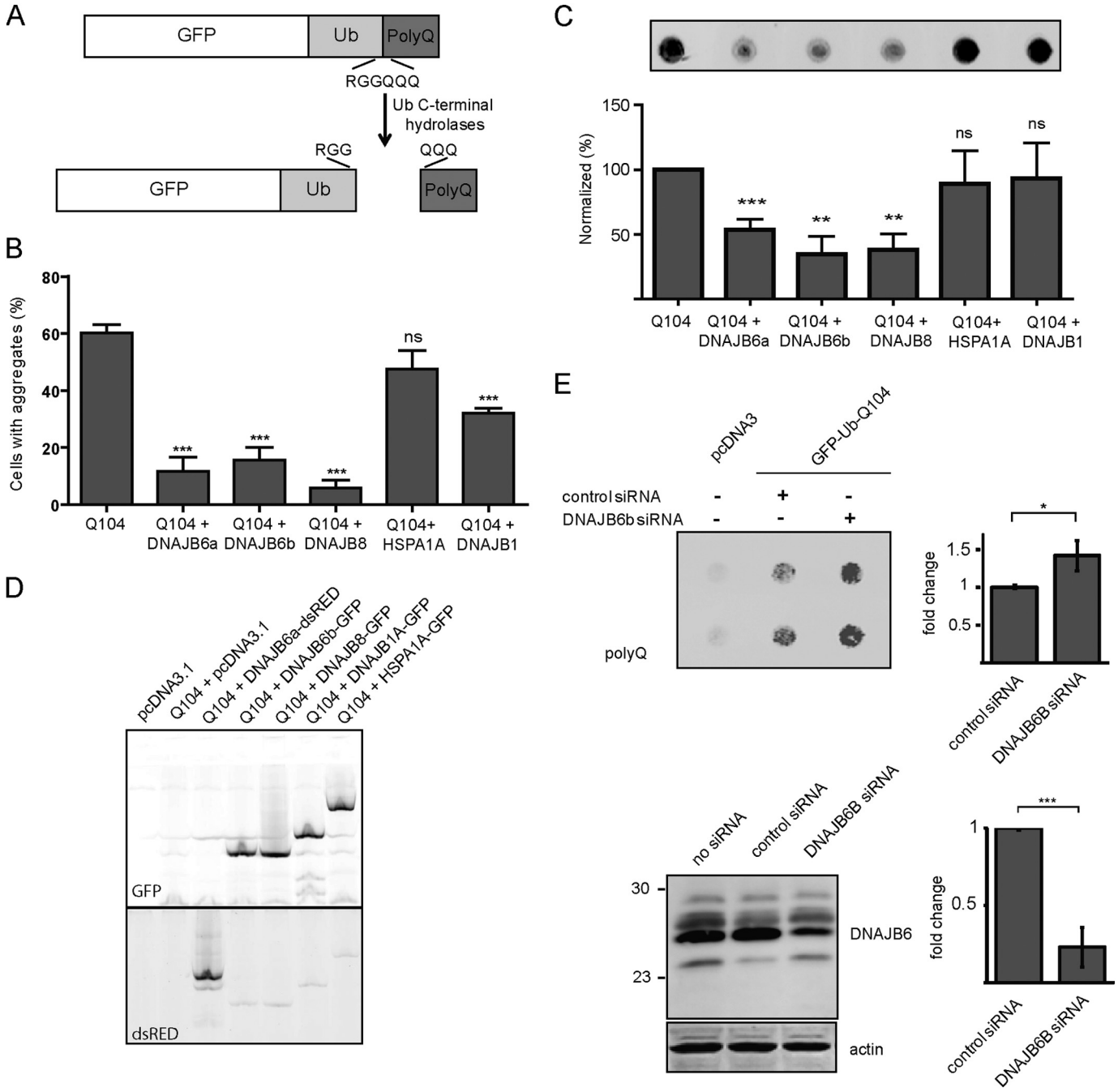

FIGURE 1. **DNAJB6 and DNAJB8 reduce aggregation of expanded polyQ peptides.** *A*, schematic representation of the cleavage of GFP-Ub-polyQ constructs by Ub C-terminal hydrolases directly after Ub, thereby separating GFP-Ub and polyQ. *B*, the percentage of the fluorescent HEK293 cells that contained fluorescent aggregates at 72 h after transfection with GFP-Ub-Q104 in combination with DNAJB6a, DNAJB6b, DNAJB8, HSPA1A, or DNAJB1, respectively. Data are mean ± S.E. of three independent experiments (two-tailed unpaired Student's *t* test). *, $p < 0.05$; ***, $p < 0.001$; *ns*, not significant. *C*, SDS-insoluble fractions prepared 72 h after transfection with the indicated constructs and analyzed by filter trap analysis. Blots were stained for polyQ using 1C2 antibody. Data are mean ± S.E. of three independent experiments (two-tailed unpaired Student's *t* test). **, $p < 0.01$; ***, $p < 0.001$. *D*, expression levels of the GFP or dsRED-tagged chaperones coexpressed with Ub-Q104 in HEK293 cells for 72 h. No molecular weight marker is present because the fluorescence of the proteins was measured directly. *E*, *upper panel*, knockdown of DNAJB6 increases aggregation in cells expressing Ub-Q104, as analyzed by filter trap analysis 72 h after transfection. *Lower panel*, knockdown of DNAJB6 by siRNA leads to a reduction in endogenous DNAJB6 levels. Data are mean ± S.E. of three independent experiments (two-tailed unpaired Student's *t* test). *, $p < 0.05$; ***, $p < 0.001$.

the following: $E = (1 - (\tau_{DA}/\tau_D)) \times 100\%$, in which τ_{DA} is the fluorescence lifetime of the donor in the presence of the acceptor (*i.e.* samples labeled with both FlAsH or GFP and ReAsH) and τ_D is the fluorescence lifetime of the donor (*i.e.* FlAsH only or GFP only) in the absence of the acceptor. Frequency domain FLIM yields a phase lifetime (τ_π) and a modulation lifetime (τ_M). Because τ_π is more sensitive than τ_M, FRET efficiency was calculated on the basis of τ_π.

Immunoblotting—Cells were trypsinized and lysed in lysis buffer (50 mM Tris/HCl (pH 7.4), 150 mM NaCl, 1 mM EDTA, 1% Triton X-100). Total cell lysates were boiled for 10 min at 99 °C with 1× Laemmli sample loading buffer (350 mM Tris/

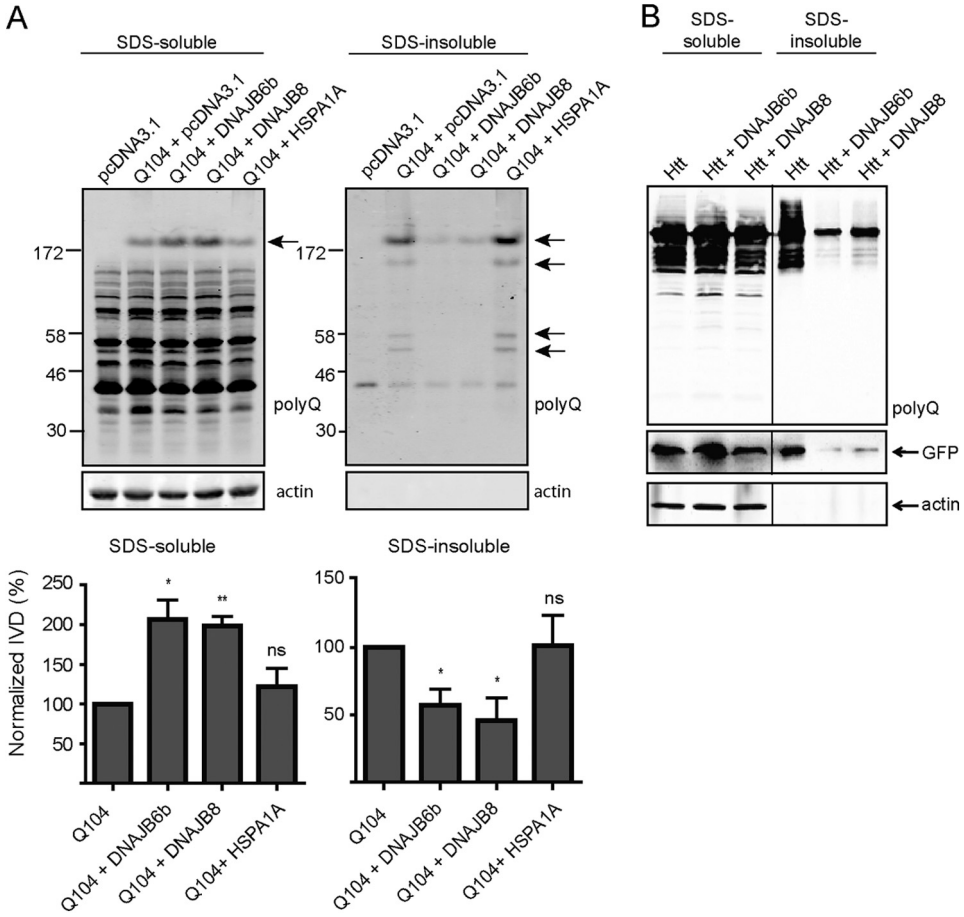

FIGURE 2. **DNAJB6 and DNAJB8 reduce insoluble levels of expanded polyQ peptides and Htt-exon-1.** *A*, SDS-soluble and SDS-insoluble fractions prepared 24 h after transfection with GFP-Ub-Q104 in combination with DNAJB6b and DNAJB8 and analyzed by Western blotting. Blots were stained for polyQ using 1C2 antibody and anti-actin antibody. The *arrows* indicate specific Glu-104 peptide bands that are quantified together in the *lower panel*. Data are mean ± S.E. of three independent experiments (two-tailed unpaired Student's *t* test). **, $p < 0.01$; ***, $p < 0.001$; *ns*, not significant. *B*, SDS-soluble and SDS-insoluble fractions prepared 72 h after transfection with Htt-exon-1-Q103-GFP in combination with DNAJB6b and DNAJB8 and analyzed by Western blotting. The blots were stained for polyQ using 1C2 antibody (*upper panel*), anti-GFP antibody (*center panel*), and anti-actin antibody (*lower panel*).

HCl (pH 6.8), 10% SDS, 30% glycerol, 6% β-mercaptoethanol, bromphenol blue), fractionated by SDS-PAGE gel electrophoresis, and transferred to a PVDF membrane (0.45-μm pore size, Schleicher & Schuell). Membranes were blocked with 5% milk, incubated with primary antibodies (anti-polyQ 1C2, 1:1000, Millipore, catalog no. MAB1574), polyclonal rabbit anti-GFP (1:1000, provided by J. Neefjes, NKI, The Netherlands), and anti-β-actin (1:1000, Santa Cruz Biotechnology, Inc., catalog no. SC-130656) and subsequently incubated with secondary antibodies (IRDye 680 or IRDye 800, 1:10,000, Licor Biosciences). The infrared signal was detected using the Odyssey imaging system (Licor Biosciences). Soluble and insoluble fractionation was performed as described before (37). Briefly, cells were lysed in 1× TEX buffer (70 mM Tris/HCl (pH 6.8), 1.5% SDS, 20% glycerol). After sonification, 50 mM DTT was added, and samples were centrifuged at 14,000 rpm at room temperature. The pelleted fraction was incubated with 100% formic acid at 37 °C for 40 min and evaporated by using a speedvac system (Eppendorf). 1× TEX buffer supplemented with 0.05% bromphenol blue was added to the pellet, and the soluble and insoluble fractions were loaded on an SDS-PAGE gel.

Filter Trap Assay—The filter retardation assay was performed as described before (38). Briefly, HEK293T cells expressing GFP-Ub-Q65 together with DNAJB6b or DNAJB8 for 72 h incubated with the various inhibitors were lysed for 30 min on ice in Nondinet P-40 (Nonidet P-40) buffer (100 mM TrisHCl (pH 7.5), 300 mM NaCl, 2% Nonidet P-40, 10 mM EDTA (pH 8.0) supplemented with complete mini protease inhibitor mixture (Roche) and phosphatase inhibitor mixture (Sigma). After 15 min of centrifugation at 14,000 rpm at 4 °C, cell pellets were resuspended in benzonase buffer (1 mM $MgCl_2$, 50 mM Tris-HCl (pH 8.0)) and incubated for 1 h at 37 °C with 250U benzonase (Merck). Reactions were stopped by adding 2× termination buffer (40 mM EDTA, 4% SDS, 100 mM DTT). Aliquots of 30 μg of protein extract were diluted into 2% SDS buffer (2% SDS, 150 mM NaCl, 10 mM Tris (pH 8.0)) and filtered through a 2-μm cellulose acetate membrane (Schleicher & Schuell) pre-equilibrated in 2% SDS buffer. Filters were washed twice with 0.1% SDS buffer (0.1% SDS, 150 mM NaCl, 10 mM Tris (pH 8.0)) and subsequently blocked in 5% dry milk in TBS. Captured aggregates were detected by incubation with 1C2 antibody and further treated like Western blot analyses.

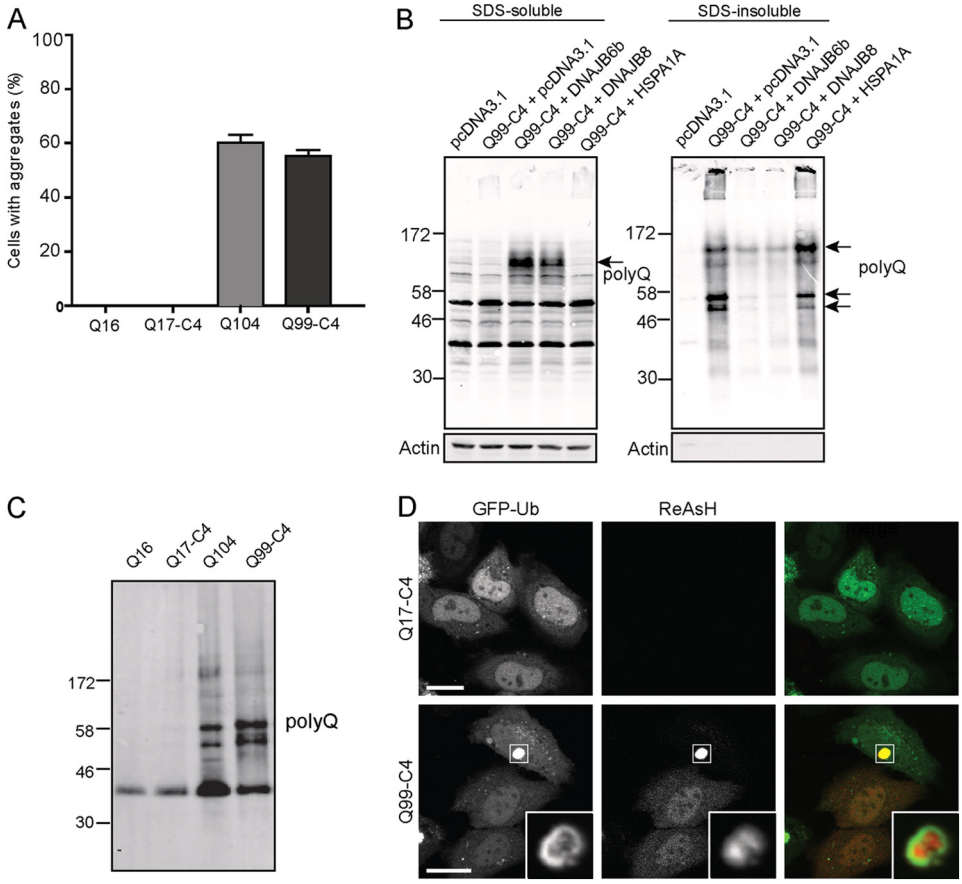

FIGURE 3. **Tetracysteine (C4)-tagged polyQ peptides behave similarly as non-labeled polyQ peptides.** *A*, the percentage of HEK293 cells containing aggregates 72 h after transfection with GFP-Ub-Q16/Q104 or C4-tagged GFP-Ub-Q17/Q99. Data are mean ± S.E. of three independent experiments. Similar amounts of aggregates were detected with either non-tagged or C4-tagged polyQ peptides. *B*, SDS-soluble and SDS-insoluble fractions prepared 24 h after transfection of HEK293 cells with Ub-Q99-C4 in combination with DNAJB6b and DNAJB8 and analyzed by Western blotting. The blots were stained for polyQ (1C2) and actin. The *arrows* indicate specific Glu-104 peptide bands. *C*, SDS-insoluble fractions of HEK293 cells expressing GFP-Ub-Q16/Q104 or C4-tagged GFP-Ub-Q17/Q99 prepared 24 h after transfection were stained for polyQ. *D*, confocal microscopy images of ReAsH-labeled HeLa cells expressing C4-tagged GFP-Ub-Q17 or GFP-Ub-Q99 48 h after transfection. ReAsH-positive cells were detected only when polyQ-expanded C4-tagged Glu-99 peptides were expressed (*lower panel*). The *inset* shows a GFP-Ub-decorated aggregate. *Scale bar* = 10 μm.

RESULTS

DNAJB6b and DNAJB8 Reduce Aggregation of PolyQ Peptides—To determine the effect of chaperones on polyQ peptide aggregation in living cells, we used GFP-ubiquitin-polyQ (GFP-Ub-polyQ) constructs that are immediately cleaved upon expression into GFP-Ub and polyQ peptides by Ub C-terminal hydrolases (Fig. 1*A*) (39). The resulting polyQ peptides lack any flanking amino acids, such as a starting methionine, and only expanded polyQ peptides beyond 40 glutamines induced aggregation, as quantified by the sequestration of GFP-Ub into aggregates (18). Although ~60% of cells expressing Glu-104 peptides contained aggregates after 72 h, coexpression of HSPA1A (Hsp70) had no significant effect on polyQ peptide aggregation, whereas DNAJB1 (Hsp40) slightly reduced aggregation (Fig. 1*B*). In contrast, coexpression of DNAJB6b or DNAJB8 resulted in a dramatic decrease in polyQ peptide aggregation when scoring the number of polyQ-expressing cells having aggregates (Fig. 1*B*) or by filter trap analysis (*C*) when similar levels of the different chaperones were expressed (*D*). In contrast, when endogenous DNAJB6 levels were decreased by siRNA (Fig. 1*E*, *lower panel*), aggregation of polyQ peptides increased, as indicated by filter trap analysis (*upper panel*).

To examine whether expression of DNAJB6b and DNAJB8 also reduced the amount of SDS-insoluble polyQ aggregates, cells expressing GFP-Ub-polyQ in combination with DNAJB6b or DNAJB8 were separated into SDS-soluble and SDS-insoluble fractions. Expression of Glu-104 peptides for 24 h resulted in a specific polyQ-positive band in the soluble and various bands in the insoluble fractions (Fig. 2*A*, *arrows*). Coexpression of DNAJB6b and DNAJB8 remarkably reduced the amount of polyQ peptides present in the SDS-insoluble fraction (Fig. 2*A*, *right panel*), which is in agreement with the reduced number of aggregates visualized in cells. Interestingly, the soluble fraction of Glu-104 peptides increased, (Fig. 2*A*, *left panel*), suggesting that DNAJB6b and DNAJB8 keep polyQ peptides soluble. To examine whether the SDS-soluble fraction was a precursor of one of the insoluble polyQ peptide fractions, we separated fractions at different time points after transfection. Both the soluble and insoluble fraction decreased when cells were treated with cycloheximide to block synthesis of new polyQ peptides during the last 16 h, suggesting that the soluble fraction was not a precursor to a particular insoluble fraction (data not shown).

SDS-insoluble levels of Htt-exon1-Q103 were also decreased by coexpression of DNAJB6b or DNAJB8 (Fig. 2*B*, *right panel*). In contrast to polyQ peptides, the SDS-soluble Htt-exon1-Q103 protein levels were not affected (Fig. 2*B*, *left panel*). The observed decrease in insoluble Htt-exon-1 could, however, indicate that DNAJB6b and DNAJB8 can

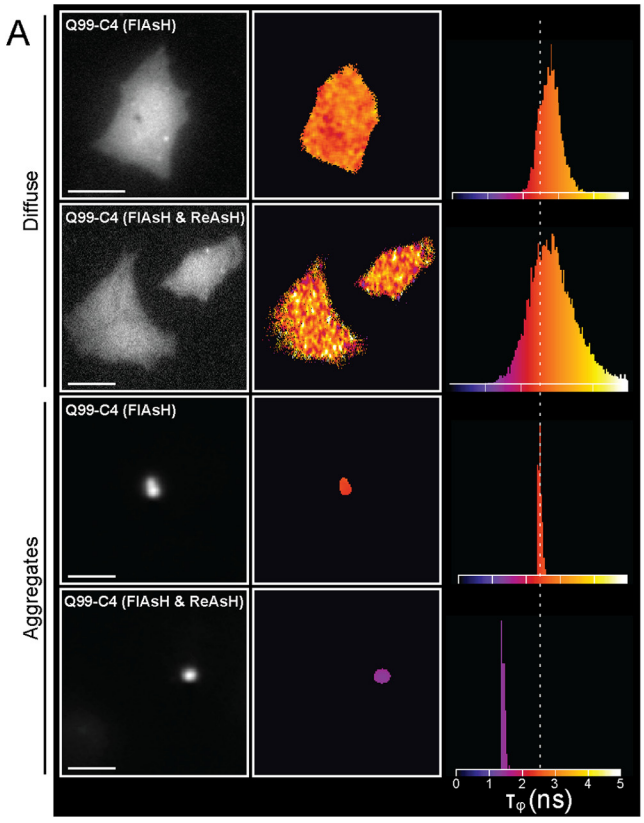

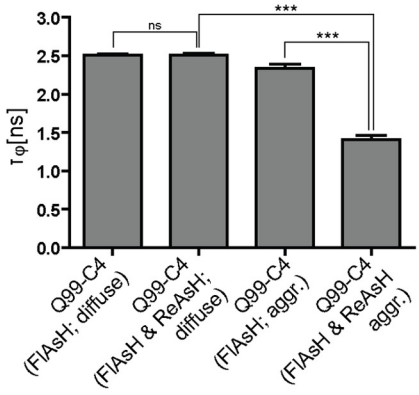

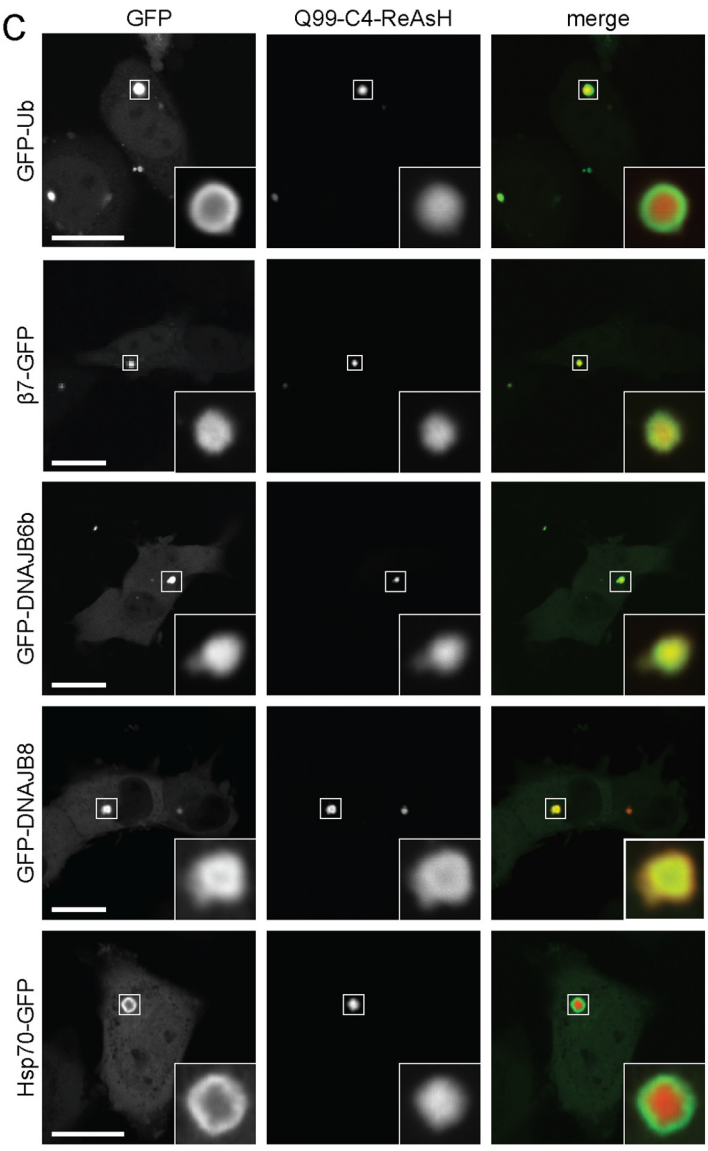

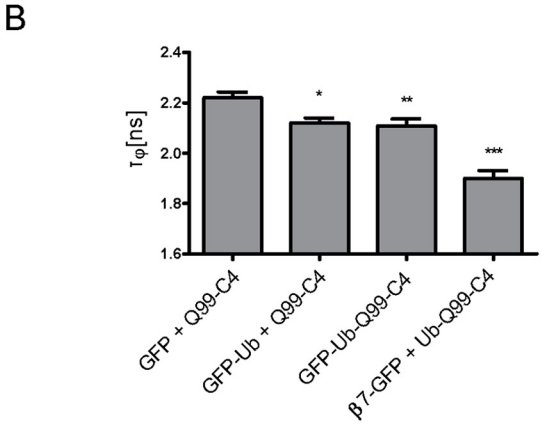

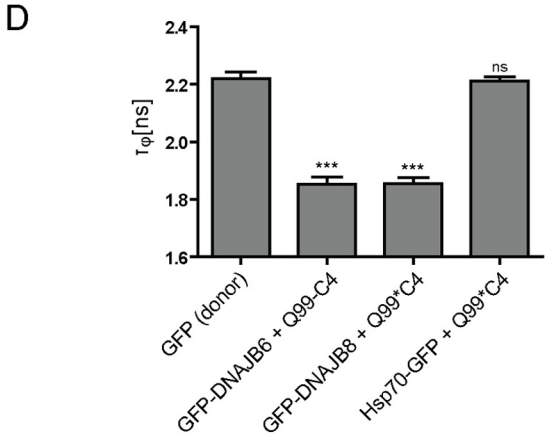

improve solubility and clearance of Htt-exon-1, as shown before (33, 40).

DNAJ6b and DNAJB8 Are Recruited into PolyQ Peptide Aggregates—To examine the effect of DNAJB6b and DNAJB8 with polyQ peptides in more detail, polyQ peptides were tagged with the small tetracysteine (C4) motif FLNCCPGCCMEP at the C terminus for direct visualization. The membrane-permeable biarsenical dye ReAsH can bind this small tag, and only then does it becomes fluorescent (34). To examine whether the C4 tag affected the behavior of polyQ peptides, we transiently expressed GFP-Ub-polyQ and GFP-Ub-polyQ-C4 peptides. Expression of either C4-tagged or non-tagged polyQ peptides resulted in a similar percentage of fluorescent cells that contained aggregates after 72 h (Fig. 3*A*). Similar to untagged Q104 peptides, DNAJB6b and DNAJB8 kept Glu-99-C4 SDS-soluble (Fig. 3*B*), and similar SDS-insoluble fractions were detected between cells expressing untagged Glu-104 or C4-tagged Glu-99 peptides (*C*). In cells without aggregates, both GFP-Ub and expanded polyQ peptides were present throughout the cytoplasm and nucleus (Fig. 3*D*, *upper panel*). However, aggregation led to the redistribution of both GFP-Ub and ReAsH-labeled Glu-99-C4, with ReAsH-labeled Glu-99-C4 sequestered in the core of aggregates and GFP-Ub in a ring around the core (Fig. 3*D*, *lower panel*, also in the *inset*). Only C4-tagged polyQ peptides of disease-related lengths accumulated and initiated aggregation, whereas short C4-tagged polyQ peptides were degraded similarly to untagged polyQ peptides.

PolyQ Peptides Sequestered in Aggregates Strongly Interact with DNAJB6b and DNAJB8—To examine whether diffuse and aggregated polyQ peptides showed intermolecular interactions, we performed FRET experiments. FRET enables sensitive evaluation of protein-protein interactions in living cells. Only when proteins are in close proximity (< 10 nm) can FRET occur and be measured (41). FLIM was used to measure FRET-FLIM, which is detected as a decrease in donor fluorescence lifetime (42). HeLa cells expressing Ub-Q99-C4 were labeled simultaneously with equal amounts of FlAsH and ReAsH at 48 h after transfection, leading to individual labeling of polyQ peptides with either FlAsH or ReAsH. When polyQ peptides were not clustered in aggregates, no reduction in FlAsH lifetime was measured (Fig. 4*A*), suggesting that polyQ-polyQ peptide interactions hardly occurred when not sequestered in aggregates. In contrast, aggregated polyQ peptides showed a remarkable decrease in lifetime of 39.6% of FlAsH, which is indicative of FRET (Fig. 4*A*). Together, these data show that polyQ peptides are mainly monomeric when not present in aggregates, whereas aggregated polyQ peptides are immobile, and only then strong polyQ-polyQ peptide interactions are observed.

The presence of GFP-Ub in aggregates most likely represents sequestered proteins that become ubiquitinated in time, whereas the polyQ peptides are not likely ubiquitinated because no lysine residues are present. Because expression of GFP-Ub-Q99-C4 results in an efficient separation of GFP-Ub and Glu-99-C4, cells expressing either GFP-Ub-Q99-C4 or GFP-Ub combined with Ub-Q99-C4 should hardly show interactions between polyQ peptides and GFP-Ub (Fig. 4*B*). The recruitment of proteasomes into the core of polyQ peptide-initiated aggregates suggests that proteasomes interact with the polyQ peptides. To substantiate this idea, cells were cotransfected with Ub-Q99-C4 and the GFP-tagged proteasomal component β7. Coexpression of ReAsH-labeled Glu-99-C4 with the GFP-tagged proteasomal component β7 caused a decreased lifetime of GFP (Fig. 4*B*), indicating a direct interaction with the polyQ peptides. In the few cells that showed aggregates upon DNAJB6b or DNAJB8 coexpression, these chaperones were present in the core of aggregates (Fig. 4*C*). Therefore, we examined whether these chaperones also interact with aggregated polyQ peptides. Both GFP-tagged DNAJB6b and DNAJB8 interacted strongly with polyQ peptides, as shown by the reduction in lifetime (Fig. 4*D*). In contrast, the recruitment of Hsp70 into polyQ peptide-induced aggregates did not result in a significantly reduced lifetime of GFP-tagged Hsp70 (Fig. 4*D*), suggesting that Hsp70 does not interact with polyQ peptides. Thus, most proteins that sequester in the core of aggregates, such as β7, DNAJB6b, and DNAJB8, interacted with aggregated polyQ peptides. This suggests that in the rare event of aggregation when DNAJB6b and DNAJB8 are coexpressed, they are trapped into aggregates induced by polyQ peptides in an early stage, which may reflect a failed function of these chaperones.

The Serine-rich Region in DNAJB6 and DNAJB8 Is Essential for Reduction of Aggregation—The DNAJ family is defined by the presence of a J domain that can regulate chaperone activity of the HSPA family by stimulating ATP hydrolysis (Fig. 5*A*) (43, 44). The HPD sequence in the J domain is essential for interaction with and accelerating the ATPase activity of HSPA (45). The other domains of DNAJ family members are involved in recognition and binding of clients and are considered to be a main factor in driving the specificity of Hsp70 machines (46). Mutating His to Glu (H31Q) in the HPD motif results in an inactive J domain (45), but this only partly impaired the ability of DNAJB6 and DNAJB8 to reduce polyQ peptide aggregation as scored by the amount of fluorescent cells having aggregates

FIGURE 4. **The chaperones DNAJB6b and DNAJB8 interact with aggregated polyQ peptides.** *A*, FLIM analysis of FlAsH in HeLa cells expressing Ub-Q99-C4 labeled with either FlAsH alone or both with FlAsH and ReAsH showing in each column, from *left* to *right*, representative *graphs* of fluorescence intensity, a false-color map of the fluorescence lifetime calculated from the phase shift (τ_φ), and a *histogram* of the lifetime distribution with the same false-color scale as the lifetime map. The *histogram* represents average phase modulation lifetimes. Only aggregated polyQ peptides showed high FRET-FLIM efficiencies. *ns*, not significant. Data are mean ± S.E. (two-tailed unpaired Student's *t* test). ***, $p < 0.001$; *ns*, not significant. *B*, FLIM analysis of GFP in HeLa cells expressing ReAsH-labeled Ub-Q99-C4 together with the indicated GFP-tagged constructs 48 h after transfection. The *histogram* represents average phase modulation lifetimes. FLIM analysis resulted in high FRET-FLIM efficiencies between aggregated Glu-99-C4 peptides and the proteasomal subunit β7. Data are mean ± S.E. (two-tailed unpaired Student's *t* test). *, $p < 0.05$; **, $p < 0.01$; ***, $p < 0.001$; *ns*, not significant. *C*, confocal microscopy images of HeLa cells expressing ReAsH-labeled Glu-99-C4 in combination with GFP-tagged DNAJB6a, DNAJB6b, or DNAJB8, which are all present in the core of the aggregate. Red fluorescent protein-tagged DNAJB1 is not recruited into aggregates, whereas red fluorescent protein-tagged HSPA1A is only recruited to the outside of the aggregate. *Scale bar* = 10 μm. *D*, FLIM analysis of GFP in cells expressing ReAsH-labeled Ub-Q99-C4 together with indicated GFP-tagged chaperones 48 h after transfection. FLIM analysis resulted in high FRET-FLIM efficiencies between aggregated polyQ peptides and DNAJB6b and DNAJB8. No FRET-FLIM was detected between aggregated polyQ peptides and Hsp70. Data are mean ± S.E. (two-tailed unpaired Student's *t* test). ***, $p < 0.001$; *ns*, not significant. *Scale bar* = 10 μm.

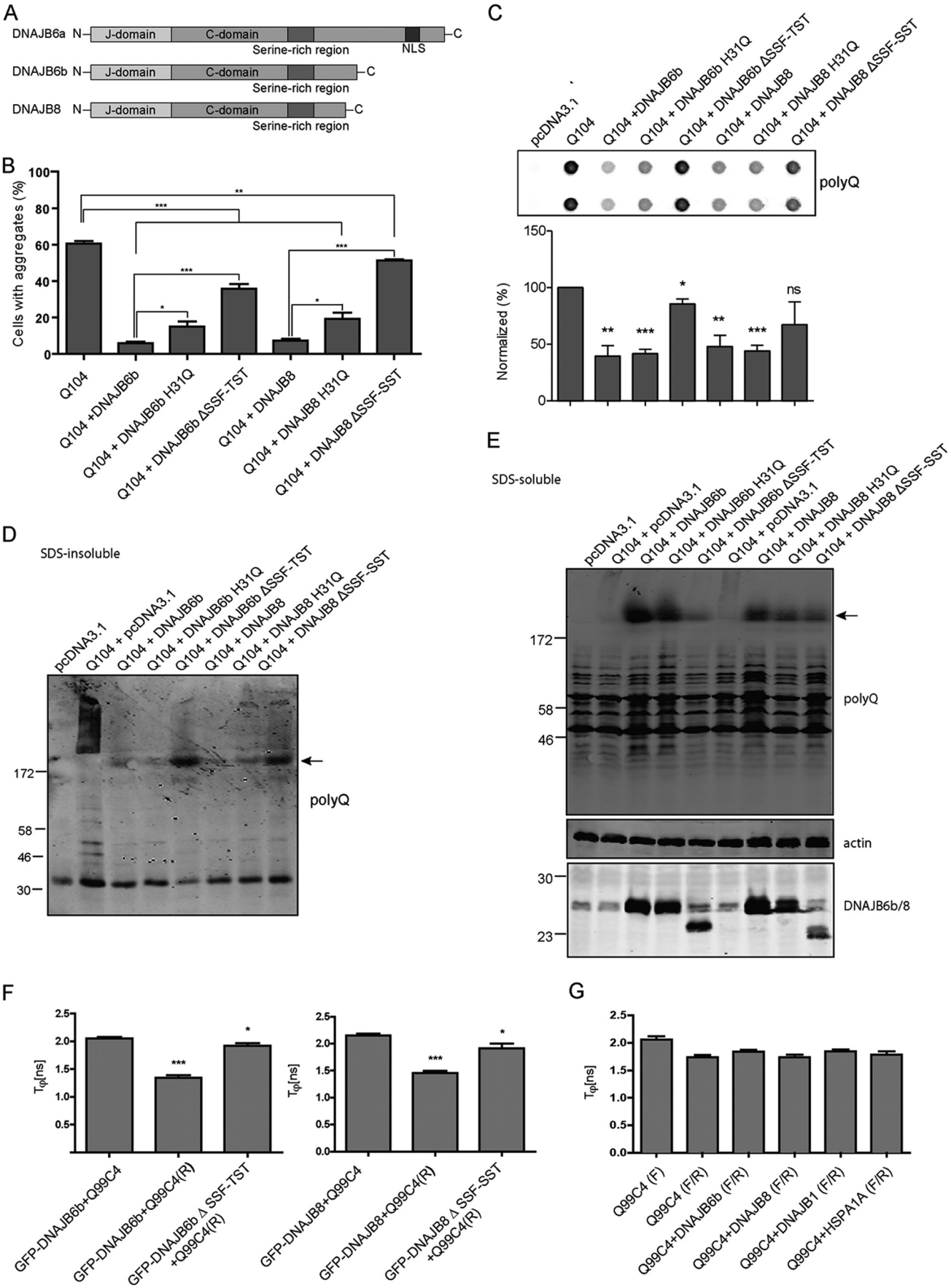

(Fig. 5*B*). The H31Q mutants also still reduced the appearance of polyQ peptides on a filter trap (Fig. 5*C*) as well as in the SDS-insoluble fraction (*D*). However, the SDS-soluble fraction was also decreased (Fig. 5*E*), indicating that the J domain is somewhat affecting DNAJB6 and DNAJB8 function, albeit that their main antiaggregation function is intact, consistent with was found before for preventing the aggregation of htt-exon-1 fragments (33).

In the C-terminal region of DNAJB6b and DNAJB8, a conserved serine-rich region (SSF-TST and SSF-SST, respectively) is present, which is absent in DNAJB1 or its related subfamily members (Fig. 5*A*) (47). Deletion of this serine-rich region was found to be crucial for DNAJB6 and DNAJB8 to interact with histone deacetylases that regulate their function as suppressors of expanded polyQ protein aggregation (33). Deletion of this serine-rich region also severely affected the ability of DNAJB6 and DNAJB8 to reduce polyQ peptide aggregation (Fig. 5*B*), resulting in more SDS-insoluble material on a filter trap (Fig. 5*C*) and Western blot analysis (*D*) and a reduction in SDS-soluble levels (*E*). The defective chaperones were still recruited into polyQ peptide aggregates, but these sequestered chaperones lost their direct interaction with the labeled polyQ peptides once the serine-rich region was disabled (Fig. 5*F*). This suggests that the sequestration of both functional and disabled DNAJB6 and DNAJB8 may not be their primary way of interfering with aggregation but, rather, reflect an inefficient attempt to prevent aggregate initiation and growth.

Because DNAJB6 and DNAJB8 strongly reduce aggregation of polyQ peptides and interact with polyQ peptides in the core of aggregates, these interactions may affect aggregation of polyQ peptides directly. To examine whether chaperones were able to reduce the strong interactions observed between polyQ peptides, we coexpressed Glu-99-C4 peptides in combination with DNAJB6, DNAJB8, Hsp40, or Hsp70. Double-labeling of C4-tagged Glu-99 peptides with FlAsH and ReAsH resulted in a high FRET-FLIM efficiency (Fig. 5*G*). Coexpression of DNAJB6b or DNAJB8 hardly affected interactions between aggregated polyQ peptides, indicating that the sequestration of DNAJB 6 or DNAJB8 does not interfere with peptide interactions within the aggregate. Similarly, Hsp40 and Hsp70 did also not affect the interactions between aggregated polyQ peptides.

Nuclear DNAJB6a Reduces Aggregation in the Cytoplasm and Nucleus—The effect of DNAJB6b on SDS-soluble levels of polyQ peptides suggests that it may counteract very early oligomerization steps of these aggregation-prone peptides. To examine this phenomenon in more detail, we reasoned that only monomeric or small oligomers can shuttle freely through the nuclear pore by diffusion. If correct, the presence of DNAJB6 in the nucleus or cytoplasm only should then reduce aggregation in both compartments by keeping the polyQ peptides soluble. DNAJB6 has two isoforms. DNAJB6b is present in both the cytoplasm and nucleus, whereas DNAJB6a contains a putative nuclear localization signal and is, therefore, localized in the nucleus only (Fig. 6*A*) (33). Despite the exclusive localization of DNAJB6a in the nucleus, the expression of DNAJB6a was as effective as DNAJB6b and DNAJB8 in reducing polyQ-peptide aggregation (Fig. 1*B*). Interestingly, the reduction in aggregate formation was not limited to the compartment were these chaperones were residing. Coexpression of DNAJB8 did not alter the ratio of nuclear and cytoplasmic aggregates after 48 h, whereas coexpression of DNAJB6b resulted in a slight change in this ratio in favor of nuclear aggregates (Fig. 6*B*, *upper panel*). Expression of DNAJB6b and DNAJB8 resulted in an even higher percentage of aggregates present in nuclei after 72 h (Fig. 6*B*, *lower panel*). The nuclear localization of DNAJB6a did not lead to the exclusive presence of aggregates in the cytoplasm because the ratio of nuclear and cytoplasmic aggregates remained unaltered after expression of DNAJB6a (Fig. 6*B*). It is concluded that although DNAJB6a is present in the nucleus only, it does not exclusively reduce aggregation in the nuclear compartment.

Together, these data suggest that DNAJB6 and DNAJB8 are efficient in targeting earlier stages of aggregation, whereas the observed recruitment of DNAJB6 and DNAJB8 into aggregates reflects sequestration of these chaperones without any effect on improved clearance. To examine whether DNAJB6a, DNAJB6b, and DNAJB8 were able to dissociate from the core of aggregates, we studied the mobility of the sequestered chaperones using fluorescent recovery after photobleaching and fluorescence loss in photobleaching analysis (48, 49). Fluorescent recovery was observed of HSPA1A but not of DNAJB6a, DNAJB6b, and DNAJB8 (Fig. 6*C*). When the entire cell was bleached repeatedly, with the exception of one fluorescent aggregate, fluorescence loss in the aggregate was measured of HSPA1A, whereas DNAJB6a, DNAJB6b, and DNAJB8 present in the core of aggregates were hardly affected by bleaching (Fig. 6*D*). These data show that DNAJB6a, DNAJB6b, and DNAJB8 were sequestered irreversibly in the core of polyQ-induced

FIGURE 5. **The serine-rich region within DNAJB6 and DNAJB8 is essential for reduction of polyQ peptide-induced aggregation.** *A*, schematic representation of domains present in DNAJB6a, DNAJB6b, and DNAJB8. *NLS*; nuclear localization signal. *B*, the percentage of fluorescent HEK293 cells that contained aggregates 72 h after transfection with GFP-Ub-Q104 in combination with DNAJB6b or DNAJB8 and their J domain (*H31Q*) and serine-rich region mutants (Δ*SSF-TST* and Δ*SSF-SST*, respectively). Data are mean ± S.E. of three independent experiments (two-tailed unpaired Student's *t* test). *, $p < 0.05$; **, $p < 0.01$; ***, $p < 0.001$. An inactive J domain induced a small increase in aggregation, whereas deletion of the serine-rich region severely increased aggregation of Glu-104 peptides. *C*, SDS-insoluble fractions prepared 72 h after transfection of HEK293 cells with he indicated constructs and analyzed by filter trap analysis. The blots were stained for polyQ using 1C2 antibody. Data are mean ± S.E. of three independent experiments (two-tailed unpaired Student's *t* test). **, $p < 0.01$; ***, $p < 0.001$; *ns*, not significant. *D*, Western blot analysis of the SDS-insoluble fraction of HEK cells expressing GFP-Ub-Q104 in combination with DNAJB6b or DNAJB8 and their mutants for 24 h. Western blot analyses were stained for polyQ with 1C2 antibody. The *arrows* indicate specific Glu-104 peptide bands. *E*, Western blot analysis of the SDS-soluble fraction of HEK293 cells expressing GFP-Ub-Q104 in combination with DNAJB6b or DNAJB8 and their mutants for 24 h. Western blot analyses were stained for polyQ with 1C2 antibody, anti-actin antibody (*center panel*), or anti-DNAJB6b/8 antibody (*lower panel*). The *arrows* indicate specific Glu-104 peptide bands. *F*, FLIM analysis of GFP-tagged DNAJB6b and the serine-rich region mutant (*upper panel*) and GFP-tagged DNAJB8 and the serine-rich region mutant (*lower panel*) in cells expressing ReAsH-labeled Ub-Q99-C4 48 h after transfection shows high FRET-FLIM efficiencies between aggregated polyQ peptides and DNAJB6b or DNAJB8, but much less FRET-FLIM was detected between aggregated polyQ peptides and their serine-rich region mutant counterparts. Data are mean ± S.E. (two-tailed unpaired Student's *t* test). *, $p < 0.05$; ***, $p < 0.001$. *Scale bar* = 10 μm. *G*, DNAJB6 or DNAJB8 do not reduce intermolecular interactions between aggregated polyQ peptides. The *histogram* represents average phase modulation lifetimes of FlAsH in HeLa cells expressing Ub-Q99-C4 together with the indicated constructs and labeled with both FlAsH and ReAsH 48 h after transfection.

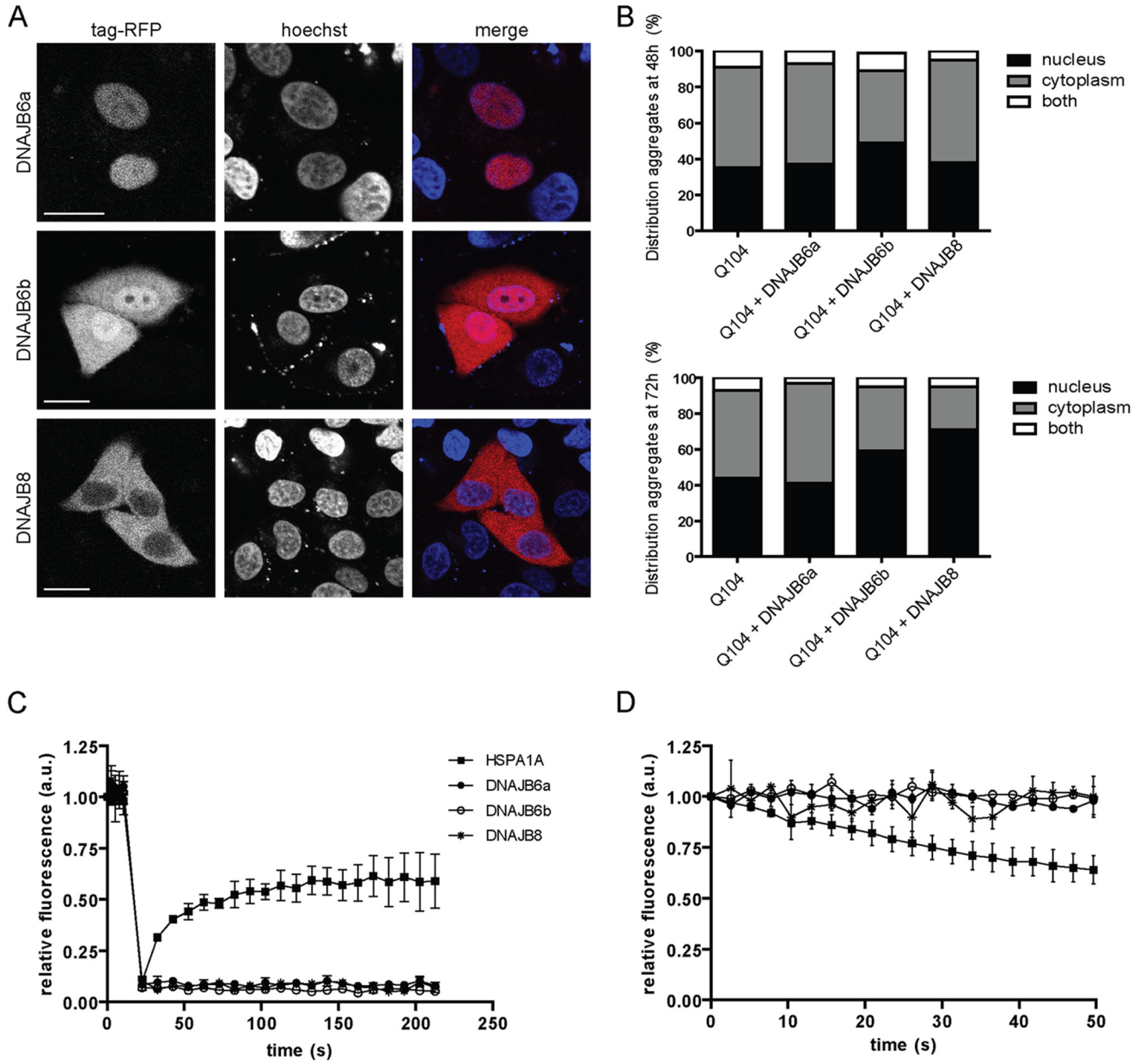

FIGURE 6. **DNAJB6 and DNAJB8 prevent aggregation of Glu-104 peptides by keeping them soluble.** *A*, confocal microscopy images of HeLa cells transfected with DNAJB6a, DNAJB6b, or DNAJB8, respectively, stained with Hoechst, and fixed 72 h after transfection. *Scale bar* = 10 μm. *B*, the ratio of aggregates present in the cytoplasm, nucleus, or both compartments 72 h after transfection with GFP-Ub-Q104 in combination with DNAJB6a, DNAJB6b, or DNAJB8, respectively, in Mel JuSo cells. Data are mean ± S.E. of three independent experiments. Chaperones did not specifically reduce aggregation in the compartment where they reside. *C*, fluorescent recovery after photobleaching analysis shows that DNAJB6a, DNAJB6b, and DNAJB8 did not recover after photobleaching, whereas HSPA1A fluorescent levels recovered. *D*, fluorescence loss of aggregates was measured using fluorescence loss in photobleaching analysis by repetitive photobleaching of another part of the cytoplasm. Fluorescence loss of HSPA1A was observed, whereas fluorescent levels of DNAJB6a, DNAJB6b, and DNAJB8 were not affected.

aggregates, indicating that once the activity of these chaperones has failed to prevent aggregation, they are irreversibly trapped in the inert core of aggregates.

DISCUSSION

Intracellular polyQ clearance may be facilitated by HSPs that prevent the formation of insoluble aggregation, allowing clearance pathways involving proteases and autophagic pathways to remove hazardous fragments. In this study, we examined mechanisms to prevent aggregation of polyQ fragments, focusing on expanded polyQ peptides that can initiate aggregation and toxicity. We found that the DNAJ family members DNAJB6 and DNAJB8 were efficient suppressors of polyQ peptide aggregation. Interestingly, detergent-soluble levels of mutant Htt-exon-1 were not affected by DNAJB6, whereas the level of soluble polyQ peptides was increased. Apparently, these chaperones prevent aggregation of polyQ peptides, leading to improved clearance of polyQ peptides, whereas soluble Htt-exon-1 is not affected. The solubilized polyQ peptides might be more efficiently cleared than Htt-exon-1 fragments. Alternatively, aggregation of Htt-exon-1 might be initiated by smaller fragments derived from Htt-exon-1 that are subsequently tar-

geted by DNAJB6. In contrast to polyQ peptides, fluorescently tagged, expanded polyQ proteins, such as Htt-exon1-GFP, were not present in the core of aggregates but sequestered in a ring around the aggregate (18, 25, 50–52). This suggests that smaller fragments containing the polyQ tract initiate aggregation and that the original GFP-tagged polyQ proteins are sequestered in a later stage. Still, it remains to be resolved whether polyQ peptides are generated in cells that express polyQ-expanded proteins, similar to *in vitro* conditions (16). This will, however, be a challenging task because the generated polyQ peptides will either be captured by DNAJB6 or DNAJB8 and/or degraded or initiate aggregation and subsequent sequestration of the original polyQ protein. To address the first option, we purified DNAJB6 from polyQ fragment-expressing cells to detect putatively associated polyQ peptides. Although we did find several peptide fragments associated with them, suggesting they indeed could be "peptide chaperones," polyQ peptides could unfortunately not be detected because of the limitations of polyQ analysis by mass spectrometry (data not shown).

DNAJB6 and DNAJB8 are the first examples of HSPs that reduce aggregation of pure polyQ peptides. Our data are supported by recent observations by the group of Cecilia Emanuelsson,[4] who showed that purified DNAJB6 and DNAJB8 can directly bind to and highly efficiently suppress polyQ peptide fibrillation initiated by soluble, pure polyQ peptides. In fact, DNAJB6 and DNAJB8 were better at suppressing fibrillation when initiated by polyQ peptides than when initiated by Htt-exon-1 fragments.[4] Given that in cells the two DNAJB proteins can prevent aggregation of Htt-exon-1 fragments (33) (this work), this implies that although some HSPs (HSPA1 or DNAJB1) might prevent sequestration of polyQ proteins into aggregates, DNAJB6 and DNAJB8 reduce aggregation of expanded polyQ peptides. Thereby they prevent that polyQ peptides can act as nucleators of aggregation and subsequent sequestering of larger polyQ-containing fragments, such as Htt-exon-1. Consistent with this model, DNAJB6 and DNAJB8 were trapped in the core of aggregates together with polyQ peptides, whereas expanded polyQ proteins and HSPA1A or DNAJB1 were absent from the core. The recruitment of HSPA1A to the outer ring of aggregates may, in fact, be due to its recognition of sequestered, possibly unfolded proteins and its attempt to solubilize these proteins. Indeed, HSPA1A, unlike DNAJB6 and DNAJB8, was not trapped in these aggregates (reflecting a failed function to prevent aggregate seeding) but showed a high degree of dynamics at the aggregate ring (Fig. 6*C*) (24). Together, this indicates that only DNAJB6 and DNAJB8 may be able to directly prevent aggregation of polyQ proteins by directly interacting with the expanded polyQ repeat, whereas most other chaperones are mostly preventing the sequestration of other proteins in the aggregate. As a result, improving the activity or protein levels of these DNAJB chaperones might delay or even prevent the aggregation of polyQ fragments, enabling intracellular clearance pathways to target and degrade these fragments.

[4] C. Månsson, V. Kakkar, E. Monsellier, Y. Sourigues, J. Härmark, H. H. Kampinga, R. Melki, and C. Emanuelsson, submitted for publication.

DNAJB6 and DNAJB8 may keep polyQ fragments soluble, whereby they may be maintained in a degradation-competent state. It remains to be established whether these chaperones can also control their degradation by targeting them to particular proteases, such as the proteasome or the puromycin-sensitive peptidase (PSA), or toward autophagosomes. Intriguingly, the ability of nuclear DNAJB6a to reduce polyQ peptide aggregation was not restricted to the nuclear compartment because aggregation within the cytoplasm was reduced similarly. This suggests that DNAJB6a keeps polyQ peptides in a soluble intermediate, which allows these peptides to freely translocate between the cytoplasm and nucleus. This is of importance because the autophagic machinery is present in the cytoplasmic compartment only (53, 54). This may also explain our observation that the ratio of cytoplasmic *versus* nuclear aggregates decreased in time because cytoplasmic aggregates may be more efficiently cleared as compared with aggregates in the nucleus.

Deletion of the serine-rich region within DNAJB6 and DNAJB8 abolished the antiaggregation properties of these chaperones. This suggests that this region is essential to recognize polyQ peptides and to inhibit their aggregation. An active J domain was less important for DNAJB6b and DNAJB8 antiaggregation properties, although it affected the soluble levels of polyQ peptides. Because the J domain is known to interact with HSPA1A and stimulates its ATPase activity (43, 44), DNAJB6 and DNAJB8 do not seem to require HSPA1A to reduce polyQ peptide aggregation. Little is known about the function of the serine-rich region in DNAJB6 and DNAJB8, although this region is suggested to be involved in DNAJB6/8 oligomerization and histone deacetylase binding (33). Also, purified DNAJB6 and DNAJB8 form large polydispersed oligomers,[4] which might be crucial for efficient polyQ peptide binding. Previous studies showed that DNAJB6 is highly enriched in the central nervous system (40, 47) and colocalizes to Lewy bodies and aggregates induced by Htt-exon-1 (40, 55). However, expression of DNAJB8 is restricted to the testes (47). Therefore, DNAJB6 may be the best candidate for potential therapeutic approaches in the fight against polyQ disorders, for example by inducing endogenous DNAJB6 expression. A combination of solubilizing polyQ peptides by expression of DNAJB6 and stimulating their subsequent degradation seems to be the most attractive alternative.

Acknowledgments—We thank Marcel Raspe for contributions to the experiments and Jurre Hageman (University Medical Center Groningen, Groningen, The Netherlands) for providing the DNAJB6 and DNAJB8 constructs.

REFERENCES

1. Orr, H. T., and Zoghbi, H. Y. (2007) Trinucleotide repeat disorders. *Annu. Rev. Neurosci.* **30,** 575–621
2. DiFiglia, M., Sapp, E., Chase, K. O., Davies, S. W., Bates, G. P., Vonsattel, J. P., and Aronin, N. (1997) Aggregation of huntingtin in neuronal intranuclear inclusions and dystrophic neurites in brain. *Science* **277,** 1990–1993
3. Goti, D., Katzen, S. M., Mez, J., Kurtis, N., Kiluk, J., Ben-Haïem, L., Jenkins, N. A., Copeland, N. G., Kakizuka, A., Sharp, A. H., Ross, C. A., Mouton, P. R., and Colomer, V. (2004) A mutant ataxin-3 putative-cleavage fragment in brains of Machado-Joseph disease patients and transgenic mice is

cytotoxic above a critical concentration. *J. Neurosci.* **24,** 10266–10279
4. Lunkes, A., Lindenberg, K. S., Ben-Haïem, L., Weber, C., Devys, D., Landwehrmeyer, G. B., Mandel, J. L., and Trottier, Y. (2002) Proteases acting on mutant huntingtin generate cleaved products that differentially build up cytoplasmic and nuclear inclusions. *Mol. Cell* **10,** 259–269
5. Cooper, J. K., Schilling, G., Peters, M. F., Herring, W. J., Sharp, A. H., Kaminsky, Z., Masone, J., Khan, F. A., Delanoy, M., Borchelt, D. R., Dawson, V. L., Dawson, T. M., and Ross, C. A. (1998) Truncated N-terminal fragments of huntingtin with expanded glutamine repeats form nuclear and cytoplasmic aggregates in cell culture. *Hum. Mol. Genet.* **7,** 783–790
6. Ellerby, L. M., Hackam, A. S., Propp, S. S., Ellerby, H. M., Rabizadeh, S., Cashman, N. R., Trifiro, M. A., Pinsky, L., Wellington, C. L., Salvesen, G. S., Hayden, M. R., and Bredesen, D. E. (1999) Kennedy's disease. Caspase cleavage of the androgen receptor is a crucial event in cytotoxicity. *J. Neurochem.* **72,** 185–195
7. Graham, R. K., Deng, Y., Slow, E. J., Haigh, B., Bissada, N., Lu, G., Pearson, J., Shehadeh, J., Bertram, L., Murphy, Z., Warby, S. C., Doty, C. N., Roy, S., Wellington, C. L., Leavitt, B. R., Raymond, L. A., Nicholson, D. W., and Hayden, M. R. (2006) Cleavage at the caspase-6 site is required for neuronal dysfunction and degeneration because of mutant huntingtin. *Cell* **125,** 1179–1191
8. Haacke, A., Broadley, S. A., Boteva, R., Tzvetkov, N., Hartl, F. U., and Breuer, P. (2006) Proteolytic cleavage of polyglutamine-expanded ataxin-3 is critical for aggregation and sequestration of non-expanded ataxin-3. *Hum. Mol. Genet.* **15,** 555–568
9. Ikeda, H., Yamaguchi, M., Sugai, S., Aze, Y., Narumiya, S., and Kakizuka, A. (1996) Expanded polyglutamine in the Machado-Joseph disease protein induces cell death *in vitro* and *in vivo*. *Nat. Genet.* **13,** 196–202
10. Merry, D. E., Kobayashi, Y., Bailey, C. K., Taye, A. A., and Fischbeck, K. H. (1998) Cleavage, aggregation and toxicity of the expanded androgen receptor in spinal and bulbar muscular atrophy. *Hum. Mol. Genet.* **7,** 693–701
11. Young, J. E., Gouw, L., Propp, S., Sopher, B. L., Taylor, J., Lin, A., Hermel, E., Logvinova, A., Chen, S. F., Chen, S., Bredesen, D. E., Truant, R., Ptacek, L. J., La Spada, A. R., and Ellerby, L. M. (2007) Proteolytic cleavage of ataxin-7 by caspase-7 modulates cellular toxicity and transcriptional dysregulation. *J. Biol. Chem.* **282,** 30150–30160
12. Bailey, C. K., Andriola, I. F., Kampinga, H. H., and Merry, D. E. (2002) Molecular chaperones enhance the degradation of expanded polyglutamine repeat androgen receptor in a cellular model of spinal and bulbar muscular atrophy. *Hum. Mol. Genet.* **11,** 515–523
13. Iwata, A., Nagashima, Y., Matsumoto, L., Suzuki, T., Yamanaka, T., Date, H., Deoka, K., Nukina, N., and Tsuji, S. (2009) Intranuclear degradation of polyglutamine aggregates by the ubiquitin-proteasome system. *J. Biol. Chem.* **284,** 9796–9803
14. Jana, N. R., Dikshit, P., Goswami, A., Kotliarova, S., Murata, S., Tanaka, K., and Nukina, N. (2005) Co-chaperone CHIP associates with expanded polyglutamine protein and promotes their degradation by proteasomes. *J. Biol. Chem.* **280,** 11635–11640
15. Rousseau, E., Kojima, R., Hoffner, G., Djian, P., and Bertolotti, A. (2009) Misfolding of proteins with a polyglutamine expansion is facilitated by proteasomal chaperones. *J. Biol. Chem.* **284,** 1917–1929
16. Venkatraman, P., Wetzel, R., Tanaka, M., Nukina, N., and Goldberg, A. L. (2004) Eukaryotic proteasomes cannot digest polyglutamine sequences and release them during degradation of polyglutamine-containing proteins. *Mol. Cell* **14,** 95–104
17. Wilburn, B., Rudnicki, D. D., Zhao, J., Weitz, T. M., Cheng, Y., Gu, X., Greiner, E., Park, C. S., Wang, N., Sopher, B. L., La Spada, A. R., Osmand, A., Margolis, R. L., Sun, Y. E., and Yang, X. W. An antisense CAG repeat transcript at JPH3 locus mediates expanded polyglutamine protein toxicity in Huntington's disease-like 2 mice. *Neuron* **70,** 427–440
18. Raspe, M., Gillis, J., Krol, H., Krom, S., Bosch, K., van Veen, H., and Reits, E. (2009) Mimicking proteasomal release of polyglutamine peptides initiates aggregation and toxicity. *J. Cell Sci.* **122,** 3262–3271
19. Marsh, J. L., Walker, H., Theisen, H., Zhu, Y. Z., Fielder, T., Purcell, J., and Thompson, L. M. (2000) Expanded polyglutamine peptides alone are intrinsically cytotoxic and cause neurodegeneration in *Drosophila*. *Hum. Mol. Genet.* **9,** 13–25
20. Chai, Y., Koppenhafer, S. L., Shoesmith, S. J., Perez, M. K., and Paulson, H. L. (1999) Evidence for proteasome involvement in polyglutamine disease. Localization to nuclear inclusions in SCA3/MJD and suppression of polyglutamine aggregation *in vitro*. *Hum. Mol. Genet.* **8,** 673–682
21. Cummings, C. J., Mancini, M. A., Antalffy, B., DeFranco, D. B., Orr, H. T., and Zoghbi, H. Y. (1998) Chaperone suppression of aggregation and altered subcellular proteasome localization imply protein misfolding in SCA1. *Nat. Genet.* **19,** 148–154
22. Holmberg, C. I., Staniszewski, K. E., Mensah, K. N., Matouschek, A., and Morimoto, R. I. (2004) Inefficient degradation of truncated polyglutamine proteins by the proteasome. *EMBO J.* **23,** 4307–4318
23. Kazantsev, A., Preisinger, E., Dranovsky, A., Goldgaber, D., and Housman, D. (1999) Insoluble detergent-resistant aggregates form between pathological and nonpathological lengths of polyglutamine in mammalian cells. *Proc. Natl. Acad. Sci. U.S.A.* **96,** 11404–11409
24. Kim, S., Nollen, E. A., Kitagawa, K., Bindokas, V. P., and Morimoto, R. I. (2002) Polyglutamine protein aggregates are dynamic. *Nat. Cell Biol.* **4,** 826–831
25. Matsumoto, G., Kim, S., and Morimoto, R. I. (2006) Huntingtin and mutant SOD1 form aggregate structures with distinct molecular properties in human cells. *J. Biol. Chem.* **281,** 4477–4485
26. Suhr, S. T., Senut, M. C., Whitelegge, J. P., Faull, K. F., Cuizon, D. B., and Gage, F. H. (2001) Identities of sequestered proteins in aggregates from cells with induced polyglutamine expression. *J. Cell Biol.* **153,** 283–294
27. Esser, C., Alberti, S., and Höhfeld, J. (2004) Cooperation of molecular chaperones with the ubiquitin/proteasome system. *Biochim. Biophys. Acta* **1695,** 171–188
28. Hartl, F. U., and Hayer-Hartl, M. (2002) Molecular chaperones in the cytosol. From nascent chain to folded protein. *Science* **295,** 1852–1858
29. Kampinga, H. H. (1993) Thermotolerance in mammalian cells. Protein denaturation and aggregation, and stress proteins. *J. Cell Sci.* **104,** 11–17
30. Nollen, E. A., Brunsting, J. F., Roelofsen, H., Weber, L. A., and Kampinga, H. H. (1999) *In vivo* chaperone activity of heat shock protein 70 and thermotolerance. *Mol. Cell. Biol.* **19,** 2069–2079
31. Fink, A. L. (1999) Chaperone-mediated protein folding. *Physiol. Rev.* **79,** 425–449
32. Vos, M. J., Hageman, J., Carra, S., and Kampinga, H. H. (2008) Structural and functional diversities between members of the human HSPB, HSPH, HSPA, and DNAJ chaperone families. *Biochemistry* **47,** 7001–7011
33. Hageman, J., Rujano, M. A., van Waarde, M. A., Kakkar, V., Dirks, R. P., Govorukhina, N., Oosterveld-Hut, H. M., Lubsen, N. H., and Kampinga, H. H. (2010) A DNAJB chaperone subfamily with HDAC-dependent activities suppresses toxic protein aggregation. *Mol. Cell* **37,** 355–369
34. Martin, B. R., Giepmans, B. N., Adams, S. R., and Tsien, R. Y. (2005) Mammalian cell-based optimization of the biarsenical-binding tetracysteine motif for improved fluorescence and affinity. *Nat. Biotechnol.* **23,** 1308–1314
35. van Munster, E. B., and Gadella, T. W. (2005) Fluorescence lifetime imaging microscopy (FLIM). *Adv. Biochem. Eng. Biotechnol.* **95,** 143–175
36. van Munster, E. B., and Gadella, T. W., Jr. (2004) Suppression of photobleaching-induced artifacts in frequency-domain FLIM by permutation of the recording order. *Cytometry A.* **58,** 185–194
37. Carra, S., Seguin, S. J., Lambert, H., and Landry, J. (2008) HspB8 chaperone activity toward poly(Q)-containing proteins depends on its association with Bag3, a stimulator of macroautophagy. *J. Biol. Chem.* **283,** 1437–1444
38. Wanker, E. E., Scherzinger, E., Heiser, V., Sittler, A., Eickhoff, H., and Lehrach, H. (1999) Membrane filter assay for detection of amyloid-like polyglutamine-containing protein aggregates. *Methods Enzymol.* **309,** 375–386
39. Johnson, E. S., Ma, P. C., Ota, I. M., and Varshavsky, A. (1995) A proteolytic pathway that recognizes ubiquitin as a degradation signal. *J. Biol. Chem.* **270,** 17442–17456
40. Chuang, J. Z., Zhou, H., Zhu, M., Li, S. H., Li, X. J., and Sung, C. H. (2002) Characterization of a brain-enriched chaperone, MRJ, that inhibits Huntingtin aggregation and toxicity independently. *J. Biol. Chem.* **277,** 19831–19838
41. Miyawaki, A. (2003) Visualization of the spatial and temporal dynamics of intracellular signaling. *Dev. Cell* **4,** 295–305

42. Van Munster, E. B., and Gadella, T. W., Jr. (2004) phiFLIM. A new method to avoid aliasing in frequency-domain fluorescence lifetime imaging microscopy. *J. Microsc.* **213,** 29–38
43. Liberek, K., Marszalek, J., Ang, D., Georgopoulos, C., and Zylicz, M. (1991) *Escherichia coli* DnaJ and GrpE heat shock proteins jointly stimulate ATPase activity of DnaK. *Proc. Natl. Acad. Sci. U.S.A.* **88,** 2874–2878
44. Qiu, X. B., Shao, Y. M., Miao, S., and Wang, L. (2006) The diversity of the DnaJ/Hsp40 family, the crucial partners for Hsp70 chaperones. *Cell Mol. Life Sci.* **63,** 2560–2570
45. Tsai, J., and Douglas, M. G. (1996) A conserved HPD sequence of the J-domain is necessary for YDJ1 stimulation of Hsp70 ATPase activity at a site distinct from substrate binding. *J. Biol. Chem.* **271,** 9347–9354
46. Kampinga, H. H., and Craig, E. A. (2010) The HSP70 chaperone machinery: J proteins as drivers of functional specificity. *Nat. Rev. Mol. Cell Biol.* **11,** 579–592
47. Hageman, J., and Kampinga, H. H. (2009) Computational analysis of the human HSPH/HSPA/DNAJ family and cloning of a human HSPH/HSPA/DNAJ expression library. *Cell Stress Chaperones* **14,** 1–21
48. Lippincott-Schwartz, J., Snapp, E., and Kenworthy, A. (2001) Studying protein dynamics in living cells. *Nat. Rev. Mol. Cell Biol.* **2,** 444–456
49. Reits, E. A., and Neefjes, J. J. (2001) From fixed to FRAP. Measuring protein mobility and activity in living cells. *Nat. Cell Biol.* **3,** E145–147
50. Chai, Y., Shao, J., Miller, V. M., Williams, A., and Paulson, H. L. (2002) Live-cell imaging reveals divergent intracellular dynamics of polyglutamine disease proteins and supports a sequestration model of pathogenesis. *Proc. Natl. Acad. Sci. U.S.A.* **99,** 9310–9315
51. Stenoien, D. L., Cummings, C. J., Adams, H. P., Mancini, M. G., Patel, K., DeMartino, G. N., Marcelli, M., Weigel, N. L., and Mancini, M. A. (1999) Polyglutamine-expanded androgen receptors form aggregates that sequester heat shock proteins, proteasome components and SRC-1, and are suppressed by the HDJ-2 chaperone. *Hum. Mol. Genet.* **8,** 731–741
52. Wyttenbach, A., Carmichael, J., Swartz, J., Furlong, R. A., Narain, Y., Rankin, J., and Rubinsztein, D. C. (2000) Effects of heat shock, heat shock protein 40 (HDJ-2), and proteasome inhibition on protein aggregation in cellular models of Huntington's disease. *Proc. Natl. Acad. Sci. U.S.A.* **97,** 2898–2903
53. Reits, E., Griekspoor, A., Neijssen, J., Groothuis, T., Jalink, K., van Veelen, P., Janssen, H., Calafat, J., Drijfhout, J. W., and Neefjes, J. (2003) Peptide diffusion, protection, and degradation in nuclear and cytoplasmic compartments before antigen presentation by MHC class I. *Immunity* **18,** 97–108
54. Rubinsztein, D. C. (2006) The roles of intracellular protein-degradation pathways in neurodegeneration. *Nature* **443,** 780–786
55. Durrenberger, P. F., Filiou, M. D., Moran, L. B., Michael, G. J., Novoselov, S., Cheetham, M. E., Clark, P., Pearce, R. K., and Graeber, M. B. (2009) DnaJB6 is present in the core of Lewy bodies and is highly up-regulated in parkinsonian astrocytes. *J. Neurosci. Res.* **87,** 238–245

The DNAJB6 and DNAJB8 Protein Chaperones Prevent Intracellular Aggregation of Polyglutamine Peptides

Judith Gillis, Sabine Schipper-Krom, Katrin Juenemann, Anna Gruber, Silvia Coolen, Rian van den Nieuwendijk, Henk van Veen, Hermen Overkleeft, Joachim Goedhart, Harm H. Kampinga and Eric A. Reits

J. Biol. Chem. 2013, 288:17225-17237.
doi: 10.1074/jbc.M112.421685 originally published online April 23, 2013
